Efficiency Improvement of Hybrid Transducer-Type Ultrasonic Motor Using Lubricant

Wei Qiu, *Student Member, IEEE*, Yosuke Mizuno, Daisuke Koyama, *Member, IEEE*, and Kentaro Nakamura, *Member, IEEE*

Abstract—Ultrasonic motors have hit a bottleneck caused by low efficiency and short life, which limits their applications to some niche areas. We believe that lubrication is a promising candidate to solve these problems. In this paper, we clarify, both analytically and experimentally, that the performance of the hybrid transducer-type ultrasonic motor (HTUSM), including the transduction efficiency, can be drastically improved at large static preloads if appropriate lubricant is applied. First, simulation was performed using an equivalent circuit in dry and lubricated conditions, and the HTUSM characteristics were shown to be more desirable at high static preloads in the lubricated condition than in the dry condition. Then, we experimentally investigated the mechanical performance of the HTUSM, verifying the effect of improving the motor performance at high preloads using lubricant, which was in good agreement with the simulation results. The maximum transduction efficiency of the HTUSM was significantly enhanced from 28% in the dry condition to 68% in the lubricated condition.

I. INTRODUCTION

B ECAUSE of their attractive features, such as high torque at low speed, simple structure, and precise positioning capability [1], [2], ultrasonic motors have been extensively studied for more than two decades, replacing electromagnetic motors in some special applications. However, because ultrasonic motors are driven by the friction force between the rotor and the stator in most cases, they inherently suffer friction loss and the wear of contact materials, causing their low efficiency and short life. Reducing the friction loss to enhance the efficiency is, therefore, a significant issue for broadening the application areas of ultrasonic motors.

In ultrasonic motors, a half-cycle of the primary vibration is extracted and transmitted to the rotor with the assistance of the other vibration orthogonal to the primary vibration. The secondary vibration modulates the preload acting on the contact interface between the transducer and the rotor; then, the friction force is varied synchronously with the primary vibration. Consequently, the pri-

mary vibration is transformed into the rotary motion of the rotor. If the modulation depth in the friction force by the secondary vibration is so large that the traction to the rotor in the positive half-cycle of the vibration is much higher than the negative half-cycle, the transformation efficiency from the primary vibration to the rotary motion of the rotor is expected to exceed 80% [3]. However, in most of the previous motors, the friction control was not ideal, resulting in the limited efficiency. Some efforts have been made to improve the motor efficiency from the viewpoint of friction control by optimizing the vibration systems [4]–[6], selecting appropriate friction materials [7], [8], and developing drive/control techniques [9], [10], but the motor efficiency has not yet been sufficiently enhanced with these methods. Some new driving mechanisms for ultrasonic motors have also been developed, including a trial to change the coefficient of friction instead of modulating the preload. This was, however, extremely difficult to perform well at ultrasonic frequency [11].

Meanwhile, with the development of the traction drive techniques [12], employing lubricant, which can vary the coefficient of friction during the operation, in ultrasonic motors has been proposed [1]. Large traction force, i.e., high coefficient of friction, is obtained during the period of high preload, whereas the coefficient of friction decreases for the period of low preload, which can reduce the reverse torque without losing the traction force if the preload is high enough during the driving period.

In this paper, we investigate the mechanical characteristics of the hybrid transducer-type ultrasonic motor (HTUSM) using lubricant, and verify the effect of improving its motor efficiency. After explaining the lubrication mechanism in the HTUSM, we theoretically show that the motor characteristics in dry and lubricated conditions are distinctively different: for instance, the motor efficiency and the no-load speed are drastically enhanced at high static preloads in the lubricated condition compared with those in the dry condition. We then experimentally clarify the improvement of the motor transduction efficiency using lubricant; the maximum efficiency is enhanced from 28% in the dry condition to 68% in the lubricated condition.

II. PRINCIPLES

HTUSMs comprise two types of piezoelectric transducers composed in one stator. The torsional vibration

generates the mechanical rotational force, whereas the longitudinal vibration controls the friction force between the contact surfaces. Because of this independent driving mechanism of the two orthogonal vibration components, high controllability is achieved. The contact of the HTUSMs is not distributed, as in traveling-wave ultrasonic motors, but is area contact.

Fig. 1 describes the operating principle of an HTUSM. A rotor is pressed to a torsional-longitudinal hybrid transducer using a coil spring with a static preload F_c. In the ideal case, the longitudinal vibration is so strong that the contact duration between the rotor and the stator is less than a quarter of one vibration cycle, and the rotor and the stator are detached when their motional directions are reverse, resulting in relatively low friction loss. In the actual motors, however, it is difficult to reduce the contact duration even below one half of the cycle. In some cases, the rotor is in contact with the stator for the whole cycle. Thus, friction loss becomes high when the elliptical trajectories of the particles in the contact surface of the stator are opposite to the moving direction of the rotor, leading to the low efficiency and the wear of contact surfaces.

Employing the functionality of lubricant is one of the methods to solve the preceding problems, because it can vary the coefficient of friction during contact as a result of the change of the load on the interface, which can be explained by the Stribeck curve [13] given in Fig. 2. If no lubricant is used, i.e., in the dry condition, the coefficient of friction is constant and reverse torque occurs. In contrast, as shown in Fig. 3, the coefficient of friction varies accord-
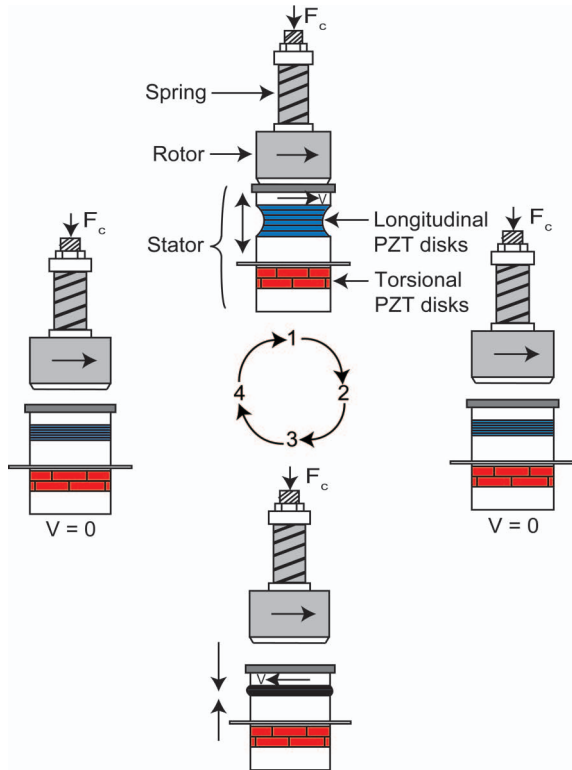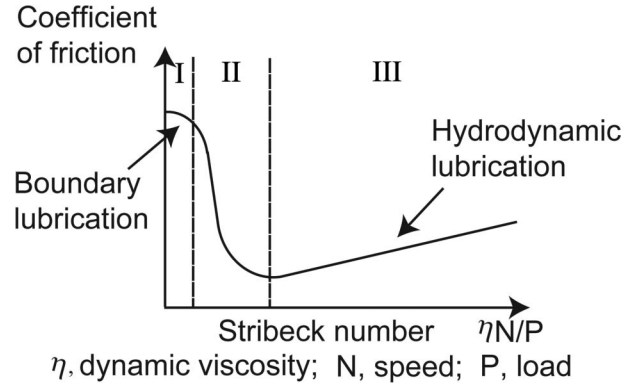

Fig. 2. Stribeck curve [13].

ing to the dynamic preload and the relative velocity when suitable lubricant is applied. The coefficient becomes high at the instance of a small slip between the rotor and the stator, or at a high preload, whereas it decreases for the period of a large slip or at a low preload. As a result, because the reverse torque is significantly suppressed, the motor efficiency is enhanced. We predict that this concept can be realized by boundary lubrication for high preloads, and hydrodynamic lubrication for low preloads.

III. SIMULATION

A. Modeling

To numerically analyze the lubrication mechanism and its effect in the HTUSM, an equivalent circuit model that simulates the torque transmission mechanism was employed, as shown in Fig. 4. The electrical and the mechanical terminals are connected by the torque factor A_τ:

$$\begin{cases} i_m = A_\tau \Omega_T, \\ \tau_0 = A_\tau V_T, \end{cases}$$

where Ω_T, i_m, τ_0, and V_T are the angular vibration velocity, the motional current, the open-circuited torque, and the driving voltage, respectively. A constant current source represents the rotor, assuming that the momentum of its inertia is infinitely large and the rotational velocity is constant. The friction characteristics in dry and lubricated conditions were separately investigated. In the dry condition, a Coulomb friction model was used, in which the torque τ is limited to the product of the coefficient of friction μ, the dynamic preload f_c, and the contact radius r, as shown in Fig. 5. On the other hand, if lubricant is applied, the coefficient of friction varies according to the change of the relative velocity between the angular vibration velocity of the stator Ω_T and the rotor rotational speed Ω_R, and the dynamic preload f_c, as corresponds to the Stribeck curve. To simulate some basic characteristics in the case in which the lubricant behaves ideally, the model for the lubricant is simplified. The fluid viscosity was assumed as a constant value because the rheology of
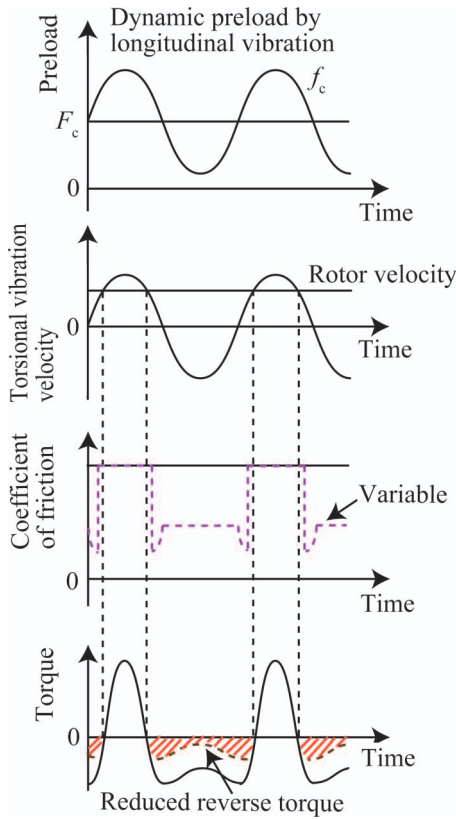

Fig. 1. Operating principle of the hybrid transducer-type ultrasonic motor.

Fig. 3. Lubrication mechanism in the hybrid transducer-type ultrasonic motor.

Fig. 5. Coulomb friction model used in calculation for the dry condition.

torque τ. The contact duration ϕ was equal to 2π. The positive torque was large during the driving period because the coefficient of friction was high as a result of the high preload and the boundary lubrication was dominant during this period. The instantaneous torque τ became negative when Ω_T was lower than Ω_R, but was followed by a sudden reduction of the reverse torque resulting from the sharp drop of the coefficient of friction in the Stribeck curve, and the hydrodynamic lubrication began to work. Through this lubrication mechanism, the reverse torque was drastically reduced without losing the traction force.

C. Motor Characteristics Versus Contact Duration

The dependence of the motor characteristics on the contact durations ϕ was examined, as shown in Figs. 9(a)–9(c). In this simulation, the static preload was assumed to be constant while the amplitude of the dynamic preload was changed to vary the contact duration. The efficiency is defined as the transduction efficiency of the HTUSM in this paper, which is the ratio of the motor output power to the input electrical power of the torsional vibrator. The maximum motor efficiency was high under short contact duration, irrespective of whether the lubricant was applied or not, because the reverse torque was extremely small as a result of the separation of the rotor and the stator.

the lubricant was not taken into account in this model. The parameters in the Stribeck curve were assumed according to the range of friction levels described in [14], as shown in Fig. 6. In this simulation, we simply defined that the time-averaged dynamic preload f_c equals the static preload F_c (see Fig. 7), following the method described in our previous papers [3], [15]. The other parameters used in this calculation are summarized in Table I.

B. Instantaneous Waveforms

The instantaneous waveforms of the HTUSM using lubricant were investigated. Fig. 8 illustrates the instantaneous variables: the torsional vibration velocity Ω_T, the rotor rotational speed Ω_R, the dynamic preload f_c, and the
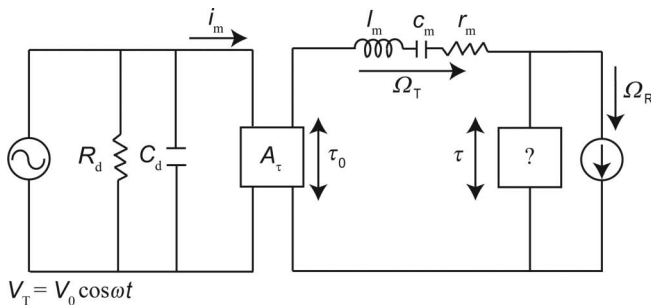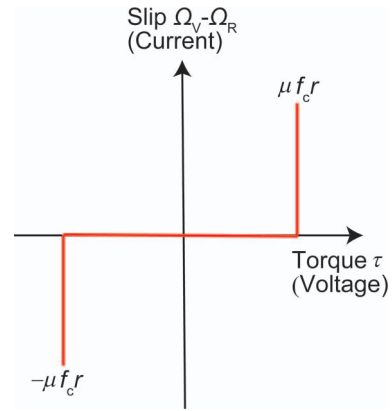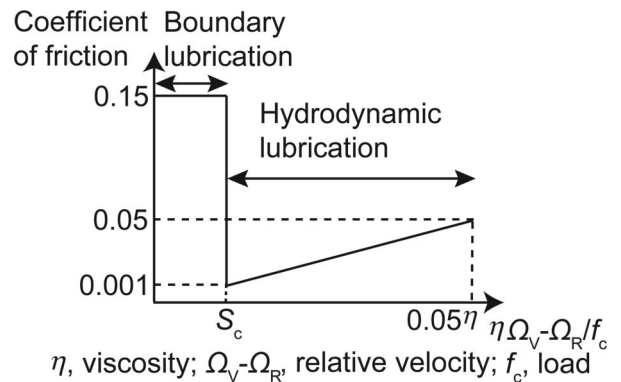
Fig. 4. Equivalent circuit of the hybrid transducer-type ultrasonic motor for torque transmission mechanism.

Fig. 6. Stribeck curve used in calculation for the lubricated condition.

Fig. 7. Waveforms of dynamic preload.

Fig. 8. Instantaneous waveforms of torsional vibration velocity Ω_T, rotational speed Ω_R, torque τ, and dynamic preload f_c.
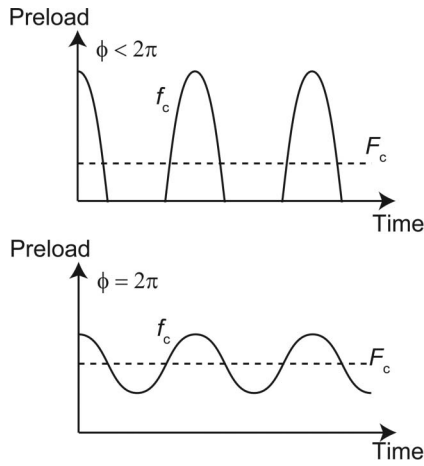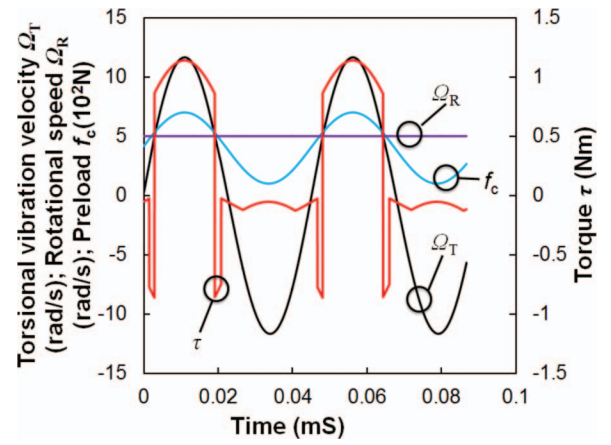
However, it is not often possible to achieve such short contact duration in actual experiments because the longitudinal vibration system is not strong enough compared with the high static preload. With the increase of the contact duration, the motor efficiency substantially decreased because large reverse torque occurred and hence the friction loss increased. In contrast, the motor efficiency was maintained at a relatively high value if lubricant was employed. The effect of the critical Stribeck number S_C on the motor performance was also investigated. In general, a large value of critical Stribeck number is not desirable for improving the motor performance as the period of the hydrodynamic lubrication becomes shorter. However, the motor efficiency decreases if S_C is extremely small because the period of the boundary lubrication is too short to keep sufficient traction force. Similar trends were found in the no-load speed and the maximum torque/contact duration curves as well.

D. Motor Characteristics Versus Static Preload

Figs. 10(a) and 10(b) indicate the effect of changing the applied voltage on the motor efficiency at various static preloads in dry and lubricated conditions. In this simulation, the amplitude of the longitudinal vibration was assumed to be constant while the static preload was changed, and the critical Stribeck number S_C was set to 0.001η. In the dry condition, the optimal static preload for the motor efficiency clearly changed at different applied voltages to the torsional vibrator. Generally, the best motor efficiency is obtained at low static preloads if the

applied voltage is low, whereas it shifts to higher static preloads if high voltage is applied. The highest value of the motor efficiency is achieved at low voltage, because the maximum efficiency is obtained under shorter contact duration. When lubricant was applied, the trends of the motor efficiency at different applied voltages were similar to those in the dry condition. However, the motor can be operated at extremely high static preloads, and the maximum efficiency at each applied voltage was higher than that without lubrication.

Figs. 11(a) and 11(b) provide the trends of the maximum torque and the no-load speed with respect to the static preload, when 500 and 300 V_{p-p} were applied, respectively. We set the critical Stribeck number S_c to 0.005η. The maximum torque with lubrication at low static preloads was smaller than that in the dry condition, because the motor was operated mainly in the hydrodynamic lubrication and the traction force was small as a result of the low coefficient of friction. However, large maximum torque was obtained at the region of high preloads, which indicates that high contact pressure is required in the lubricated condition to maintain the traction force. As for the no-load speed, with lubrication, the motor was operated at high preloads, where the motor did not rotate without lubrication.

IV. EXPERIMENTS

### A. Motor Structure and Materials

The HTUSM used in the experiment was 25 mm in diameter; it contained two 4-mm-thick torsional PZT disks and six 1-mm-thick longitudinal PZT disks, as shown in Fig. 12(a). The contact side of the rotor had a triangular cross-section and was truncated for 0.3 mm in width for contact, as shown in Fig. 12(b). Four deeply truncated parts were made as oil reservoirs to keep sufficient lubrication. The total contacting area was 5.64 mm². The friction materials for the stator and the rotor were alumina
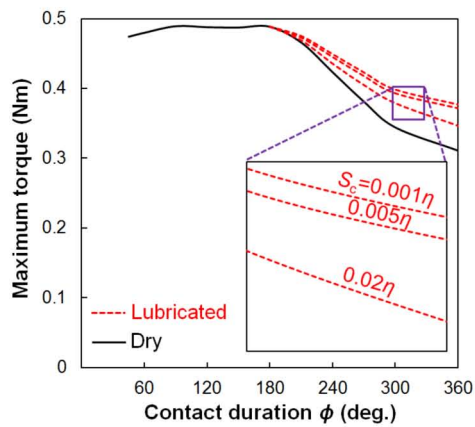
TABLE I. PARAMETERS USED IN CALCULATION.

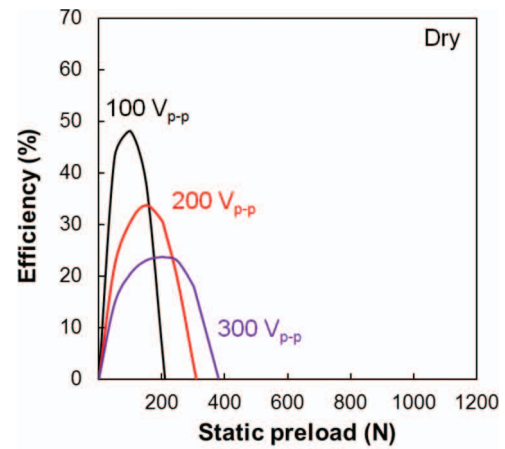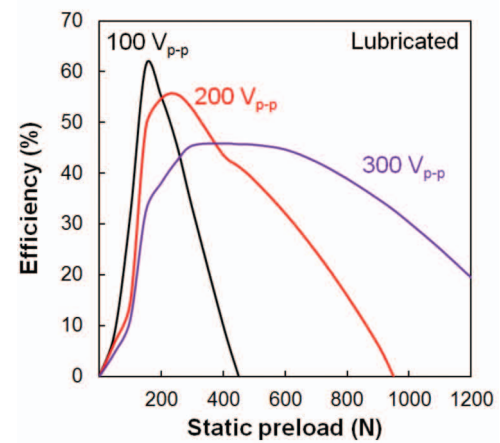|	
Torque factor A_τ	0.00377
Free admittance Y_{m0}	1.27 mS
Mechanical Q	117
Torsional resonance f_{T0}	22.1 kHz
Clamped capacitance C_d	2.3 nF
Dielectric loss R_d	100 kΩ
Contact radius r	10.85 mm
Coefficient of friction in the dry condition μ	0.15
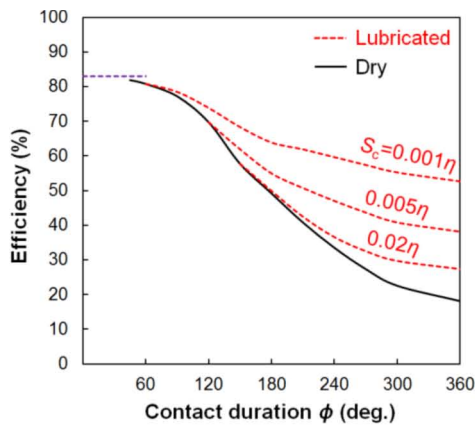
(a)
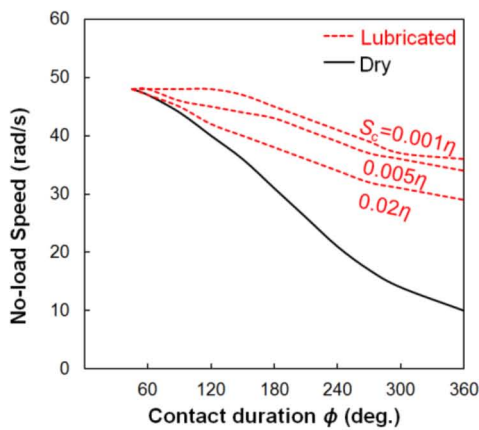
(b)

(c)

Fig. 9. Calculated dependences of (a) motor efficiency, (b) no-load speed, and (c) maximum torque on contact duration.

(a)

(b)

Fig. 10. Calculated motor efficiency as a function of the static preload in (a) dry and (b) lubricated conditions.

and silicon nitride, respectively, because severe wear still occurred even with lubrication, and wear debris was not easily transported away from the contact area when metals were used. High-traction fluid (HTRF) with 100 cSt viscosity was selected as the lubricant.

B. Experimental Setup

Fig. 13 depicts the schematic diagram of the experimental setup. A function generator with a phase shifter was employed to drive the HTUSM. The driving power was amplified with two amplifiers and transformers. Different weights were employed to obtain the load characteristics of the motor. The rotor rotational speed was measured by a high-speed digital camera (M5, Integrated Design Tools Inc., Tallahassee, FL). The electrical power to the torsional PZT disks was calculated from the definition of the effective power with the voltage and current waveforms, and also verified by a digital power meter (Power HiTESTER 3332, Hioki, Ueda, Japan).

C. Results and Discussion

The results of the experiments conducted at different static preloads in dry and lubricated conditions are shown in Figs. 14 and 15.
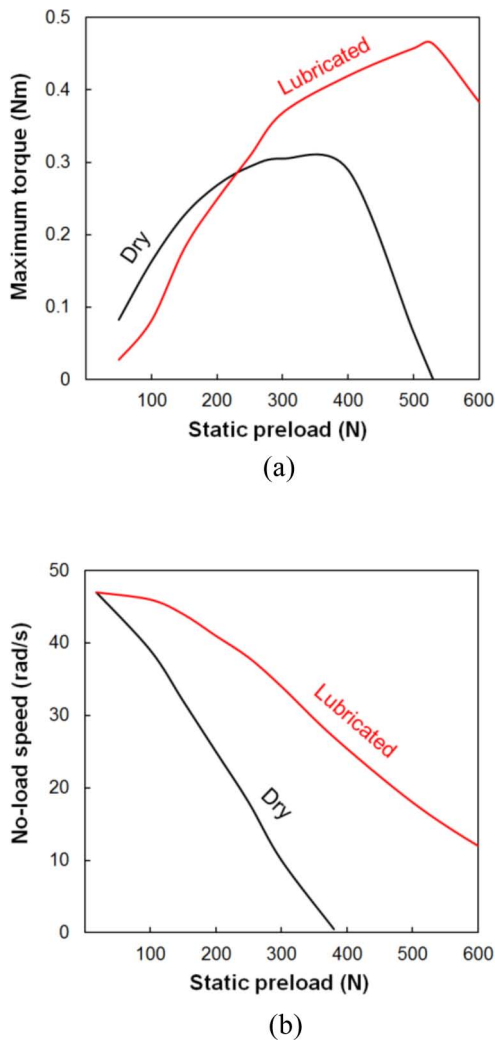
Fig. 11. Calculated dependences of (a) maximum torque and (b) no-load speed on static preload.

Fig. 12. (a) Dimension of the hybrid transducer-type ultrasonic motor used in the experiment and (b) design of the contact side of the rotor.

During the experiment, the longitudinal resonance frequency was adjusted to be close to the torsional resonance frequency. The applied voltage to the longitudinal PZT disks was fixed at 450 V_{p-p} to avoid the effect of the longitudinal vibration on the transduction efficiency. Prior to the experiment, we usually added a small quantity of lubricant, which was apparently sufficient for the daily experiment. The effects of the average contact pressure on the motor efficiency at different applied voltages to the torsional PZT disks are shown in Figs. 14(a) and (b). The average contact pressure was defined as the ratio of the static preload to the contacting area. The experimental results were in good agreement with simulation results indicating that the maximum efficiency was achieved at low static preloads if low voltage was applied. In the dry condition, the motor efficiency reached its maximum at low static preloads, where the efficiency was low with lubrication. However, without lubrication, the motor almost stopped at 13.5 MPa contact pressure even when high voltage was applied, so that the efficiency drastically decreased. In contrast,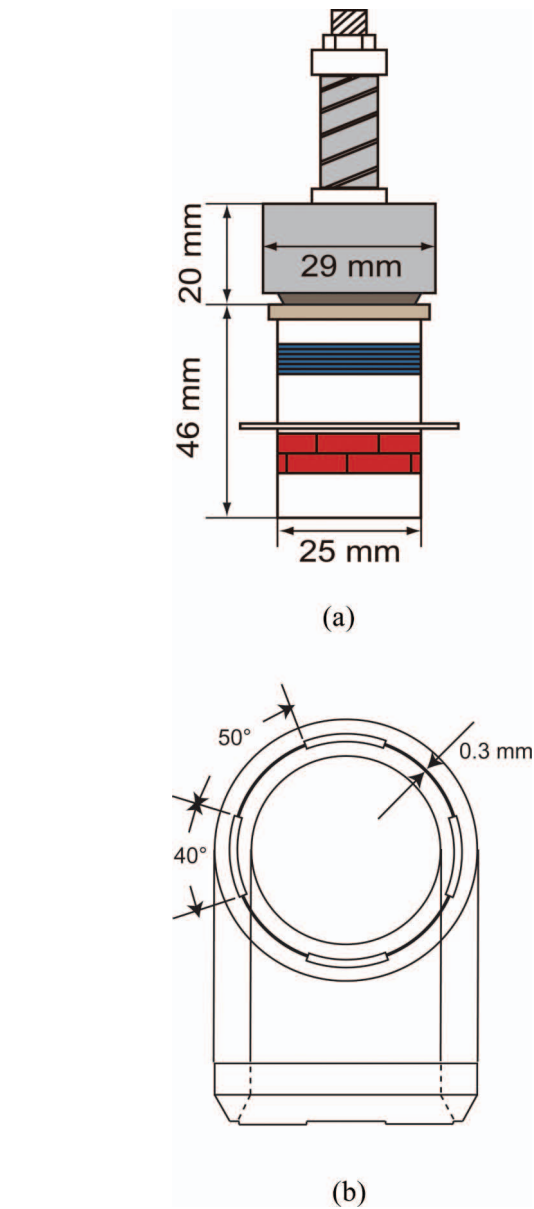 the motor efficiency was enhanced with the increasing contact pressure after lubrication. The maximum efficiency was increased from 28% in the dry condition to 68% in the lubricated condition. In addition, the motor efficiency reached 44% at 300 V_{p-p} applied voltage and 37.2 MPa contact pressure, which was the largest applicable pressure of the spring we used. Thus, the motor with lubrication operates well even under relatively high pressure, which shows that it can be utilized in applications for which high torque is required.

Figs. 15(a) and 15(b) depict the maximum torque and the no-load speed as functions of contact pressure, both at 300 V_{p-p}. When the contact pressure was low, the maximum torque in the dry condition showed clear superiority to that in the lubricated condition, and 0.3 N·m torque was obtained at 10.1 MPa contact pressure. In contrast,
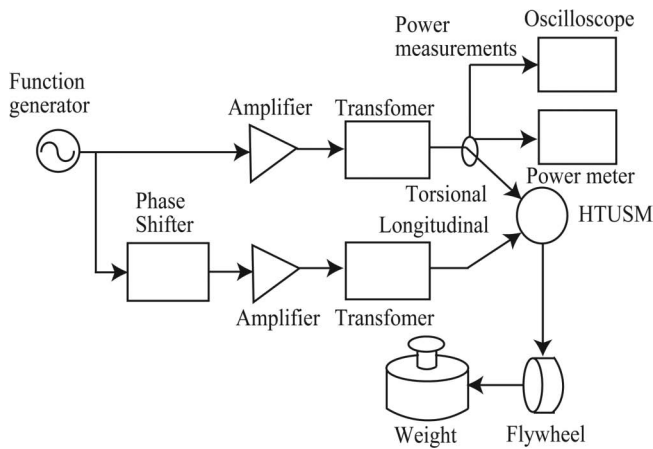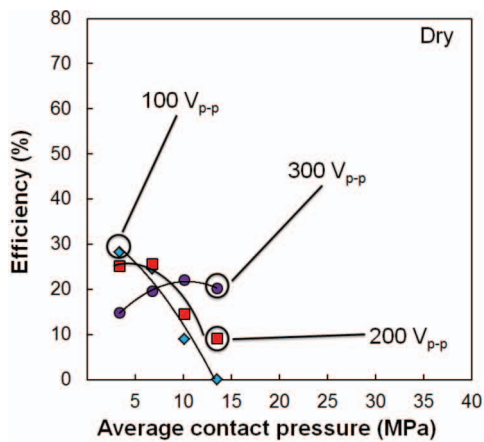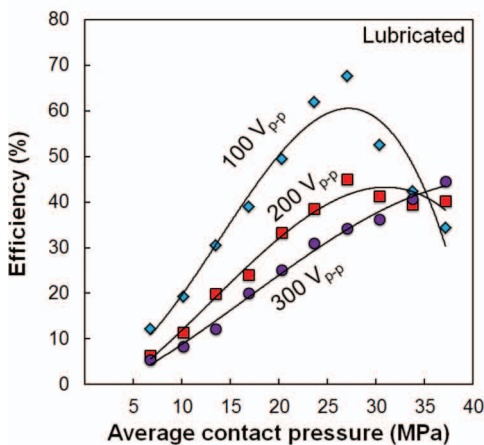
Fig. 13. Diagram of experimental setup.

as the contact pressure increased, the maximum torque increased in the lubricated condition until the maximum value of 0.36 N·m was achieved at 27.0 MPa contact pressure. When the contact pressure increased further, the maximum torque was still maintained at high values, cor-

(a)

(b)

Fig. 15. (a) Maximum torque and (b) no-load speed as functions of static preload.
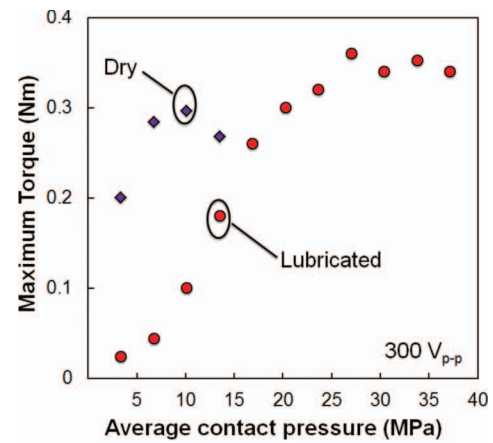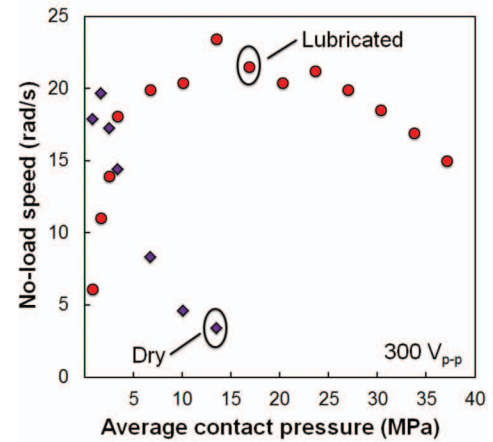

(a)

(b)

Fig. 14. Motor efficiency as a function of static preload in (a) dry and (b) lubricated condition. In the experiments, 5 MPa equals approximately 28.6 N.

responding to the high efficiency. There was a discrepancy between the simulation and the experimental results for the no-load speed. The no-load speed with lubrication was low at low static preloads, in contrast with the high no-load speed in simulation. This is probably because of the power loss in the ball bearing used in the experiment, which was neglected in simulation. Another possible reason is that the fluid connects the rotor and the stator because of its surface tension even when there is no normal force acting on the contact surfaces, which was also not simulated. The reverse torque was induced by the fluid drag even the contact duration was small, which seems to have caused the low no-load speed. Therefore, if taken into account in simulation, these factors make the no-load speed in the lubricated condition lower than in the dry condition at low preloads, where the efficiency and the maximum torque are even lower. As the contact pressure increased, the no-load speed reached the maximum, and began to decrease when the contact pressure further increased. No-load speed as high as 14.95 rad/s was achieved even at 37.2 MPa contact pressure, which is a distinctive difference between conditions with and without lubrication.

V. Conclusions

We analytically and experimentally compared the HTUSM characteristics in dry and lubricated conditions and examined the effect of improving the motor efficiency with lubrication at high static preloads. With lubrication, the motor performance at low static preloads, including the motor efficiency, the no-load speed, and the maximum torque, was lower than that without lubrication. However, it was drastically improved at high static preloads, which indicates that high pressure is required to keep sufficient traction force if lubricant is applied. The transduction efficiency of the motor was enhanced from 28% in the dry condition to 68% in the lubricated condition. Under much higher static preloads than in the dry condition, the HTUSM was operated with relatively high efficiency after being lubricated, which is desirable for high-torque usages. In addition, because the contact surfaces were well protected by the lubricant, the motor lifetime can be potentially prolonged. We believe that this study will lead to a breakthrough for broadening the application fields of ultrasonic motors.

Acknowledgments

References

[1] S. Ueha and Y. Tomikawa, *Ultrasonic Motors—Theory and Applications*. New York, NY: Oxford University Press, 1993.

[2] K. Uchino, *Piezoelectric Actuators and Ultrasonic Motors*. New York, NY: Kluwer Academic, 1997.

[3] K. Nakamura, M. Kurosawa, and S. Ueha, "Design of a hybrid transducer type ultrasonic motor," *IEEE Trans. Ultrason. Ferroelectr. Freq. Control*, vol. 40, no. 4, pp. 395–401, 1993.

[4] T. Morita, M. Kurosawa, and T. Higuchi, "Design of a cylindrical ultrasonic micromotor to obtain mechanical output," *Jpn. J. Appl. Phys.*, vol. 35, no. 5B, pp. 3251–3254, 1996.

[5] M. Aoyagi and Y. Tomikawa, "Improvement in performance of longitudinal and torsional vibrator combination-type ultrasonic motor," *Jpn. J. Appl. Phys.*, vol. 38, no. 5B, pp. 3342–3346, 1999.

[6] J. Satonobu, D. Lee, K. Nakamura, and S. Ueha, "Improvement of the longitudinal vibration system for the hybrid transducer ultrasonic motor," *IEEE Trans. Ultrason. Ferroelectr. Freq. Control*, vol. 47, no. 1, pp. 216–221, 2000.

[7] K. Nakamura, M. Kurosawa, H. Kurebayashi, and S. Ueha, "An estimation of load characteristics of an ultrasonic motor by measuring transient responses," *IEEE Trans. Ultrason. Ferroelectr. Freq. Control*, vol. 38, no. 5, pp. 481–485, 1991.

[8] K. Uchino, "Piezoelectric ultrasonic motors: Overview," *Smart Mater. Struct.*, vol. 7, no. 3, pp. 273–285, 1998.

[9] T. Ishii, T. Shinkoda, S. Ueha, K. Nakamura, and M. Kurosawa, "Efficiency improvement of an ultrasonic motor driven with rectangular waveform," *Jpn. J. Appl. Phys.*, vol. 35, no. 5B, pp. 3281–3285, 1996.

[10] T. Ishii, H. Takahashi, K. Nakamura, and S. Ueha, "A low-wear driving method of ultrasonic motors," *Jpn. J. Appl. Phys.*, vol. 38, no. 5B, pp. 3338–3341, 1999.

[11] K. Nakamura, M. Maruyama, and S. Ueha, "A new ultrasonic motor using electro-rheological fluid and torsional vibration," *Ultrasonics*, vol. 34, no. 2–5, pp. 261–264, 1996.

[12] F. W. Heilich and E. E. Shube, *Traction Drive*. New York, NY: Marcel Dekker, 1983.

[13] H. Czichos, *Tribology—A System Approach to the Science and Technology of Friction, Lubrication and Wear*. New York, NY: Elsevier Scientific, 1978.

[14] F. P. Bowden and D. Tabor, *Friction—An Introduction to Tribology*. New York, NY: Krieger, 1982.

[15] K. Nakamura, M. Kurosawa, and S. Ueha, "Characteristics of a hybrid transducer-type ultrasonic motor," *IEEE Trans. Ultrason. Ferroelectr. Freq. Control*, vol. 38, no. 3, pp. 188–193, 1991.

Wei Qiu was born in Jiangsu Province, China, on June 27, 1987. He received the B.E. degree in electrical engineering from Nantong University, Nantong, China, in 2009; the M.Sc. degree in electrical and electronic engineering from The University of Hong Kong, Hong Kong, China, in 2010; and the M.E. degree in information processing from the Tokyo Institute of Technology, Yokohama, Japan, in 2012. He is presently a doctoral candidate in the Precision and Intelligence Laboratory, Tokyo Institute of Technology, Kanagawa, Japan. His research interests include ultrasonic motors and actuators, with a particular interest on lubrication in ultrasonic motors, and chaotic mixing.

He received an award for the excellent student presentation at the annual meeting of the Acoustical Society of Japan (ASJ) in 2012. He is a student member of IEEE and ASJ.

Yosuke Mizuno was born in Hyogo, Japan, on October 13, 1982. He received the B.E., M.E., and Dr.Eng. degrees in electronic engineering from the University of Tokyo, Japan, in 2005, 2007, and 2010, respectively.

In 2004, he worked on optical information processing at the University of Tokyo. From 2005 to 2007, he was engaged in spintronics and studied spin hot-carrier transistors for his master's degree. From 2007 to 2010, he was engaged in Brillouin optical correlation-domain reflectometry at the University of Tokyo for his Dr.Eng. degree. From 2007 to 2010, he was a Research Fellow (DC1) of the Japan Society for the Promotion of Science (JSPS). From 2010 to 2012, as a Research Fellow (PD) of JSPS, he worked on polymer optics at Tokyo Institute of Technology, Japan. In 2011, he stayed at BAM Federal Institute for Materials Research and Testing, Germany, as a Visiting Research Associate. Since 2012, he has been an Assistant Professor at the Precision and Intelligence Laboratory, Tokyo Institute of Technology, where he is active in fiber-optic sensing, polymer optics, and ultrasonics.

Dr. Mizuno is the winner of the Funai Research Award 2010, the Ando Incentive Prize for the Study of Electronics 2011, and the NF Foundation R&D Encouragement Award 2012. He is a member of the Japanese Society of Applied Physics (JSAP), and the Institute of Electronics, Information, and Communication Engineers (IEICE) of Japan.

Daisuke Koyama was born in Kyoto, Japan, in September 1977. He received a Dr.Eng. degree from Doshisha University, Kyoto, Japan. He joined the Precision and Intelligence Laboratory, Tokyo Institute of Technology, as a research associate in 2005, and was promoted to assistant professor in 2007 and associate professor in 2011. He is currently an associate professor in the Faculty of Science and Engineering, Doshisha University.

He received an award for the encouragement of young scientists at the Symposium for Ultrasonic Electronics and Engineering in 2003 and the Awaya Kiyoshi Award for encouragement of research from the Acoustical Society of Japan in 2008. His main fields of research are in ultrasonic electronics, especially ultrasonic levitation in high-intensity ultrasound and applications of nonlinear microbubble vibration and destruction in medical ultrasonics. Dr. Koyama is a member of the IEEE, the Acoustical Society of Japan, and the Institute of Electrical Engineers of Japan.

Kentaro Nakamura was born in Tokyo, Japan, on July 3, 1963. He received the B.E., M.E., and Dr.Eng. degrees from the Tokyo Institute of Technology, Tokyo, Japan, in 1987, 1989, and 1992, respectively. He has been a professor of the Precision and Intelligence Laboratory, Tokyo Institute of Technology, since 2010. His research fields are the application of ultrasonics and the measurement of vibration and sound using optical methods as well as fiber optic sensors.

He received the Awaya Kiyoshi Award for encouragement of research from the Acoustical Society of Japan in 1996. He was awarded the best paper awards from the Institute of Electronics, Information and Communication Engineers in 1998 and from Ultrasonic Electronics in 2007 and 2010, respectively. He received the JJAP editorial contribution award from the Japan Society of Applied Physics in 2007. Dr. Nakamura is a member of the IEEE, and served as the vice-president of the Acoustical Society of Japan from 2010 to 2011.